CHEMISTRY
A EUROPEAN JOURNAL

Supporting Information

Mechanism and *exo* Regioselectivity of Organolanthanide-Mediated Intramolecular Hydroamination/Cyclization of 1,3-Disubstituted Aminoallenes: A Computational Study

Sven Tobisch

Institut für Anorganische Chemie der Martin-Luther-Universität Halle-Wittenberg, Fachbereich Chemie, Kurt-Mothes-Straße 2, D-06120 Halle, Germany

E-mail: tobisch@chemie.uni-halle.de

Computational Details

Method. All calculations have been performed with the program package TURBOMOLE[1] using density functional theory (DFT). The local exchange-correlation potential by Slater[2a,b] and Vosko et al.[2c] was augmented with gradient-corrected functionals for electron exchange according to Becke[2d] and correlation according to Perdew[2e] in a self-consistent fashion. This gradient-corrected density functional is usually termed BP86 in the literature and was shown to be capable of describing both energetic and structural aspects of organolanthanide compounds reliably.[3] The suitability of the BP86 functional for the reliable determination of the energy profile for organolanthanide-supported catalytic transformations has been demonstrated in previous studies,[4] and this allows mechanistic conclusions having substantial predictive value to be drawn. In view of the fact that all species investigated in this study show a large HOMO–LUMO gap, a spin-restricted formalism was used for all the calculations.

Two different basis set levels (basis set A, B) were adopted throughout the present investigation, employing the same description of the lanthanide atom. For Lu we used the Stuttgart–Dresden quasirelativistic effective core potential (SDD) with the associate (7s6p5d)/[5s4p3d] valence basis set contracted according to a (31111/3111/311) scheme.[5] This ECP treats [Kr]$4d^{10}4f^{14}$ as a fixed core, whereas $5s^25p^66s^25d^16p^0$ shells are taken into account explicitly. First, as far as basis set A is regarded, all other elements were represented by Ahlrichs' split-valence SV(P) basis set[6a] with polarization functions on heavy main group atoms, but not on hydrogen; namely, for carbon and nitrogen a 7s/4p/1d set contracted to (511/31/1) and for hydrogen a 4s set contracted to (31). The second more accurate basis set B, consists of Ahlrichs' valence triple-ζ TZVP basis set[6b] with polarization functions on all main group atoms; namely, for carbon and nitrogen a 11s/6p/1d set contracted to (62111/411/1) and for hydrogen a 5s/1p set contracted to (311/1).

Stationary Points. The geometry optimization and the saddle-point search were carried out by utilizing analytical/numerical gradients/Hessians according to standard algorithms. No symmetry constraints were imposed in any case. The stationary points located by using basis set A were identified exactly by the curvature of the potential-energy surface at these points corresponding to the eigenvalues of the Hessian. This level of basis-set quality has been identified as a reliable tool for the assessment of structural parameters and vibrational frequencies.[7] All reported transition states possess exactly one negative Hessian eigenvalue, while all other stationary points exhibit exclusively positive eigenvalues. Each transition state was further confirmed by following its imaginary vibrational mode downhill on both sides from slightly distorted TS structures, yielding to the reactant and product minima presented on the reaction profile for the individual steps. Visual inspection of imaginary vibrational modes was performed with the StrukEd program.[8] The many isomers that are possible for each of the investigated species were carefully explored. The reaction and activation enthalpies and free energies (ΔH, $\Delta H^{\ddagger}$ and ΔG, $\Delta G^{\ddagger}$ at 298 K and 1 atm) were evaluated according to standard textbook procedures[9] using harmonic frequencies that were computed at basis set A level. To obtain more accurate energy profiles, all key species were fully located by employing basis set B.

It has been explicitly scrutinized for each of the individual steps in Scheme 1 whether a specific substrate species, which are always available in excess,[10] is likely to facilitate the elementary process. Furthermore, the influence of nonspecific solute–solvent interactions[11] on the energy profile of individual steps has been estimated for benzene[10] (dielectric constant ε = 2.247 at 298 K)[12] by employing the conductor-like screening model (COSMO) due to Klamt and Schüürmann[13] as implemented in TURBOMOLE.[14] Nonelectrostatic contributions to solvation were not considered. The solvation effects were included selfconsistently in the calculations, and all key species were fully optimized including solvation at the BP86 basis set B level. The optimized atomic COSMO radii (r_H = 1.3 Å, r_C = 2.0 Å, r_N = 1.83 Å)[15] have been used, in combination with the non-optimized radius of 2.22 Å for Lu.

Energetics (BP86(COSMO)/basis set B) on the ΔH(298 K) surface were reported as ΔE plus zero point energy correction at 0 K plus thermal motion corrections at 298 K plus solvation correction. The Gibbs free-energies were obtained as $\Delta G_{298} = \Delta H_{298} - T\Delta S$ at 298 K and 1 atm. The $T\Delta S$ contribution of about 11–13 kcal mol^{-1} (under standard conditions) calculated for substrate coordination in gas phase certainly does not reflect the real entropic cost for substrate association/dissociation processes under actual catalytic conditions.[10] The difference in the reaction entropy for the Cp^*_2LnR + **1** ? Cp^*_2LnR–**1** substrate uptake process taking place in the gas and condensed phases is mainly due to the substrate solvation, since the solvation entropies of the Cp^*_2LnR species and the Cp^*_2LnR–**1** adduct can be regarded as being similar. The

solvation entropy of ethylene is about 16 cal mol^{-1} K^{-1} in typical aromatic hydrocarbon solvents,[16] which can reasonably be adopted as a rough estimate for aminoallenes as well. This reduces the entropic costs for substrate complexation by about 4.8 kcal mol^{-1} (298.15 K); thus to about two-thirds of the gas-phase value. This estimation agrees reasonably well with the findings of a recent theoretical study, where it was shown that for polar solvents the entropies in solution decrease to nearly half of the gas-phase value.[17] Therefore, the solvation entropy for substrate association and dissociation was approximated as being two-thirds of its gas-phase value, which the author considers as a reliable estimate of the entropy contribution in the condensed phase.

[1] a) R. Ahlrichs, M. Bär, M. Häser, H. Horn, C. Kölmel, C. *Chem. Phys. Lett.* **1989**, *162*, 165; b) O. Treutler, R. Ahlrichs, *J. Chem. Phys.* **1995**, *102*, 346; c) K. Eichkorn, O. Treutler, H. Öhm, M. Häser, R. Ahlrichs, *Chem. Phys. Lett.* **1995**, *242*, 652.

[2] a) P. A. M. Dirac, *Proc. Cambridge Philos. Soc.* **1930**, *26*, 376; b) J. C. Slater, *Phys. Rev.* **1951**, *81*, 385; c) S. H. Vosko, L. Wilk, M. Nussiar, *Can. J. Phys.* **1980**, *58*, 1200; d) A. D. Becke, *Phys. Rev.* **1988**, *A38*, 3098; e) J. P. Perdew, *Phys. Rev.* **1986**, *B33*, 8822; *Phys. Rev. B* **1986**, *34*, 7406.

[3] see, for instance: a) S. Tobisch, Th. Nowak, H. Boegel, *J. Organomet. Chem.* **2001**, *619*, 24; b) H. Heiber, O. Gropen, J. K. Laerdahl, O. Swang, U. Wahlgreen, *Theor. Chem. Acc.* **2003**, *110*, 118.

[4] see, for instance: a) S. Tobisch, *Chem. Eur. J.* **2005**, *11*, 3113; b) S. Tobisch, *J. Am. Chem. Soc.* **2005**, *127*, 11979.

[5] M. Dolg, H. Stoll, A. Savin, H. Preuß, *Theor. Chim. Acta* **1989**, *75*, 173.

[6] a) A. Schäfer, C. Huber, R. Ahlrichs, *J. Chem. Phys.* **1992**, *97*, 2571; b) A. Schäfer, C. Huber, R. Ahlrichs, *J. Chem. Phys.* **1994**, *100*, 5829.

[7] W. Koch, M. C. Holthausen, *A Chemist's Guide to Density Functional Theory*, 2nd ed., Wiley-VCH, Weinheim, **2001**.

[8] For further details, see: www.struked.de.

[9] D. A. McQuarrie, *Statistical Thermodynamics*, Harper & Row, New York, **1973**.

[10] a) V. M. Arredondo, F. E. McDonald, T. J. Marks, *J. Am. Chem. Soc.* **1998**, *120*, 4871.; b) V. M. Arredondo, F. E. McDonald, T. J. Marks, *Organometallics* **1999**, *18*, 1949; c) typical reaction conditions for the organolanthanide-mediated cycloamination of aminoallenes are: 40–70-fold molar excess of the substrate (for example, 4,5-heptadien-1-ylamine, **1**) together with the precatalyst (for example, $Cp^*_2LuCH(SiMe_3)_2$, **2**) at 25 °C in noncoordinating solvents, *viz.* benzene, toluene, pentane and cyclohexane.

[11] a) J. Tomasi, M. Persico, *Chem. Rev.* **1994**, *94*, 2027; b) C. J. Cramer, D. G. Truhlar, *Chem. Rev.* **1999**, *99*, 2161; c) C. J. Cramer, *Essentials of Computational Chemistry: Theories and Models*; John Wiley & Sons: Chichester, U. K., **2002**, pp 347-383.

[12] *CRC Handbook of Chemistry and Physics*, 3rd electronic ed. (Ed.: D. R. Lide), **2000**; http://www.knovel.com/.

[13] A. Klamt, G. J. Schüürmann, *Chem. Soc., Perkin Trans. 2* **1993**, 799; b) A. Klamt, In *Encyclopedia of Computational Chemistry, Vol. 1*, (Ed.: P. von R. Schleyer), Wiley, Chichester, **1998**, pp 604-615.

[14] A. Schäfer, A. Klamt, D. Sattel, J. C. W. Lohrenz, F. Eckert, F. *Phys. Chem. Chem. Phys.* **2000**, *2*, 2187.

[15] A. Klamt, V. Jonas, Th. Bürger, J. C. W. Lohrenz, *J. Phys. Chem. A* **1998**, *102*, 5074.

[16] E. Wilhelm, R. Battino, *Chem. Rev.* **1973**, *73*, 1.

[17] J. Cooper, T. Ziegler, *Inorg. Chem.* **2002**, *41*, 6614.

Table S1. Enthalpies and free energies of activation and reaction for regioisomeric 5-*exo* and 6-*endo* cyclization paths for 4,5-hexadien-1-ylamine substrate **1x**.[a,b]

cyclization pathway	precursor	TS	product
5-*exo*	0.0/*0.0* (**3x'**) 3.2/*5.2* (**3x''**)	5.9/*9.0* ($\Delta S^{\ddagger}$ = −10.6 eu)[c]	–8.1/*–5.9* (**4x)**
6-*endo*	0.0/*0.0* (**3x'**)	5.7/*8.4* ($\Delta S^{\ddagger}$ = −9.2 eu)[c]	−18.1/*–15.2* (**5x)** −16.4/*–13.0* (**5x'**)

[a] Total barriers, reaction energies and activation entropies are relative to the thermodynamically favorable isomer of **3x**, *viz*. **3x'** with a nonchelating allene functionality. [b] Enthalpies and free energies of activation ($\Delta H^{\ddagger}/\Delta G^{\ddagger}$) and reaction ($\Delta H/\Delta G$) are given in kilocalories per mole; numbers in italic type are the Gibbs free energies. [c] The activation entropy is given in entropic units ≡ cal mol^{1} K^{-1}.

Table S2. Enthalpies and free energies of activation and reaction for protonolysis of the azacycle–Lu compounds **4** and **5** by aminoallene substrate **1** to afford the cycloamine-amido–Lu compounds **6**-**8** along various regioisomeric paths for proton transfer.[a,b]

	cycloamine-generating path		
cyclization path	**4**-S/**5**-S[c]	TS	product[c]
5-*exo*			
syn pathway			2-[(*Z*)-prop-1-enyl]pyrrolidine
H-trf onto C^6 of **4s**	3.1/*12.6* (**4s**-S)[d]	10.7/*20.4* ($\Delta S^{\ddagger}$ = –32.6 eu)[e]	–10.5/*–1.7* (**6s**)
anti pathway			2-[(*E*)-prop-1-enyl]pyrrolidine
H-trf onto C^6 of **4a**	6.5/*15.3* (**4a**-S)[d]	11.6/*21.1* ($\Delta S^{\ddagger}$ = –31.9 eu)[e]	–12.7/*–3.9* (**6a**)
6-*endo*			
syn pathway			6-ethyl-tetrahydropyridine
H-trf onto C^7 of **5s**	–1.0/*7.7* (**5s**-S)	6.5/*16.1* ($\Delta S^{\ddagger}$ = –32.4 eu)[e]	–17.8/*–8.8* (**7**)
H-trf onto C^7 of **5s'**	–1.4/*8.1* (**5s'**-S)	1.8/*11.8* ($\Delta S^{\ddagger}$ = –33.3 eu)[e]	
			2-[(*Z*)-ethylidene]piperidine
H-trf onto C^5 of **5s'**	–6.0/*3.4* (**5s'**-S)[d]	–1.5/*8.6* ($\Delta S^{\ddagger}$ = –33.8 eu)[e]	–15.5/*–6.3* (**8s**)
anti pathway			6-ethyl-tetrahydropyridine
H-trf onto C^7 of **5a**	1.4/*9.8* (**5a**-S)	10.0/*19.4* ($\Delta S^{\ddagger}$ = –31.5 eu)[e]	–12.0/*–3.8* (**7**)
H-trf onto C^7 of **5a'**	5.1/*13.7* (**5a'**-S)	12.0/*21.8* ($\Delta S^{\ddagger}$ = –32.8 eu)[e]	
			2-[(*E*)-ethylidene]piperidine
H-trf onto C^5 of **5a'**	–2.2/*6.2* (**5a'**-S)[d]	11.6/*20.9* ($\Delta S^{\ddagger}$ = –31.3 eu)[e]	–10.8/*–2.0* (**8a**)

[a] Total barriers, reaction energies and activation entropies are relative to {**4s**/**4a** + **1**} and {**5s**/**5a** + **1**} for protonation of 5-*exo* and 6-*endo* cyclization intermediate, respectively. [b] Enthalpies and free energies of activation ($\Delta H^{\ddagger}/\Delta G^{\ddagger}$) and reaction ($\Delta H/\Delta G$) are given in kilocalories per mole; numbers in italic type are the Gibbs free energies. [c] See the text (or Figures 2, S5–S7) for description of the various isomers of the amine adducts **4**-S, **5**-S, and of the cycloamine-amido–Lu product species **6**–**8**. [d] The precursor amine-adduct species is not identical with the related one reported in Table 2. [e] The activation entropy is given in entropic units ≡ cal mol^{-1} K^{-1}.

Table S2 (continued). Enthalpies and free energies of activation and reaction for protonolysis of the azacycle–Lu compounds **4** and **5** by aminoallene substrate **1** to afford the cycloamine-amido–Lu compounds **6**-**8** along various regioisomeric paths for proton transfer.[a,b]

	substrate-assisted cycloamine-generating path[f]
cyclization path	TS
5-*exo*[g]	
syn – H-trf onto C^6 of **4s**	21.1/*38.6* ($\Delta S^{\ddagger}$= –58.6 eu)[e]
anti – H-trf onto C^6 of **4a**	24.1/*41.9* ($\Delta S^{\ddagger}$= –59.7 eu)[e]
5-*exo*[h]	
syn - H-trf onto C^6 of **4s**	24.6/*42.1* ($\Delta S^{\ddagger}$= –58.7 eu)[e]
anti – H-trf onto C^6 of **4a**	28.1/*45.1* ($\Delta S^{\ddagger}$= –56.9 eu)[e]
6-*endo*[g]	
syn – H-trf onto C^7 of **5s'**	14.7/*32.8* ($\Delta S^{\ddagger}$= –60.8 eu)[e]
anti – H-trf onto C^7 of **5a'**	23.3/*41.1* ($\Delta S^{\ddagger}$= –59.6 eu)[e]
syn – H-trf onto C^5 of **5s'**	11.6/*29.7* ($\Delta S^{\ddagger}$= –60.5 eu)[e]
anti – H-trf onto C^5 of **5a'**	23.6/*41.1* ($\Delta S^{\ddagger}$= –58.6 eu)[e]
6-*endo*[h]	
syn – H-trf onto C^7 of **5s'**	10.9/*28.8* ($\Delta S^{\ddagger}$= –60.0 eu)[e]
anti – H-trf onto C^7 of **5a'**	18.2/*35.9* ($\Delta S^{\ddagger}$= –59.5 eu)[e]
syn – H-trf onto C^5 of **5s'**	8.5/*26.6* ($\Delta S^{\ddagger}$= –60.4 eu)[e]
anti – H-trf onto C^5 of **5a'**	15.6/*33.5* ($\Delta S^{\ddagger}$= –59.8 eu)[e]

[a] Total barriers, reaction energies and activation entropies are relative to {**4s**/**4a** + **1**} and {**5s**/**5a** + **1**} for protonation of 5-*exo* and 6-*endo* cyclization intermediate, respectively. [b] Enthalpies and free energies of activation ($\Delta H^{\ddagger}/\Delta G^{\ddagger}$) and reaction ($\Delta H/\Delta G$) are given in kilocalories per mole; numbers in italic type are the Gibbs free energies. [c] See the text (or Figures 2, S5–S7) for description of the various isomers of the amine adducts **4**-S, **5**-S, and of the cycloamine-amido–Lu product species **6**–**8**. [d] The precursor amine-adduct species is not identical with the related one reported in Table 2. [e] The activation entropy is given in entropic units ≡ cal mol^{-1} K^{-1}. [f] The process to be assisted by an additionally coordinating aminoallene molecule has been investigated with methylamine ($MeNH_2$, S') as the substrate. Total barriers, reaction energies and activation entropies are relative to {**4s**/**4a** + **1** + $MeNH_2$} and {**5s**/**5a** + **1** + $MeNH_2$}, respectively. [g] The additive substrate acts as a Lu-coordinated spectator ligand (Figures S8–S10, top). [f] The additive substrate acts as a 'proton shuttle' (Figures S8–S10, bottom).

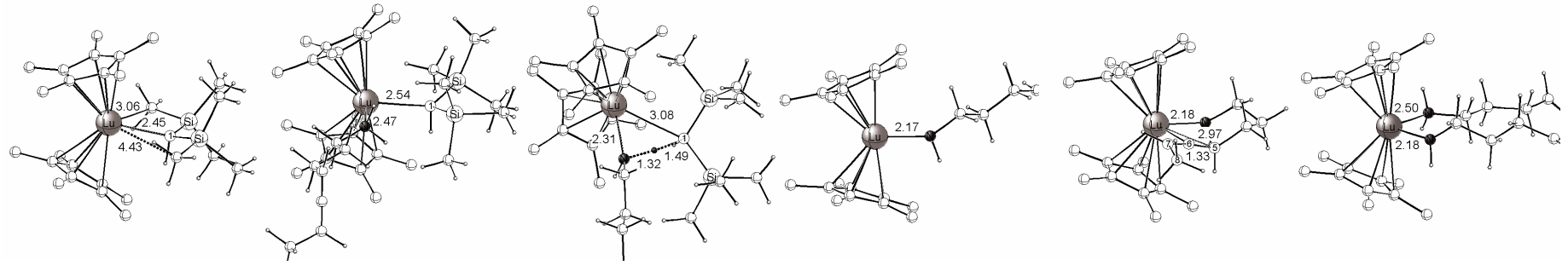

2 **2**-S TS[**1**+**2**–**3**+$CH_2(TMS)_2$] **3'** **3s''** **3'**-S

Figure S1. Selected structural parameter [Å] of the optimized structures of key species for **1** + **2** ? **3** + $CH_2(TMS)_2$ activation of precatalyst **2** through protonolysis by aminoallene substrate **1**. The cutoff for drawing Lu–C bonds was arbitrarily set to 3.1 Å. The hydrogen atoms on the methyl groups of the catalyst backbone are omitted for the sake of clarity. Please note that the amino-/amidoallene moiety and the catalyst's backbone are displayed in a truncated fashion for several of the species.

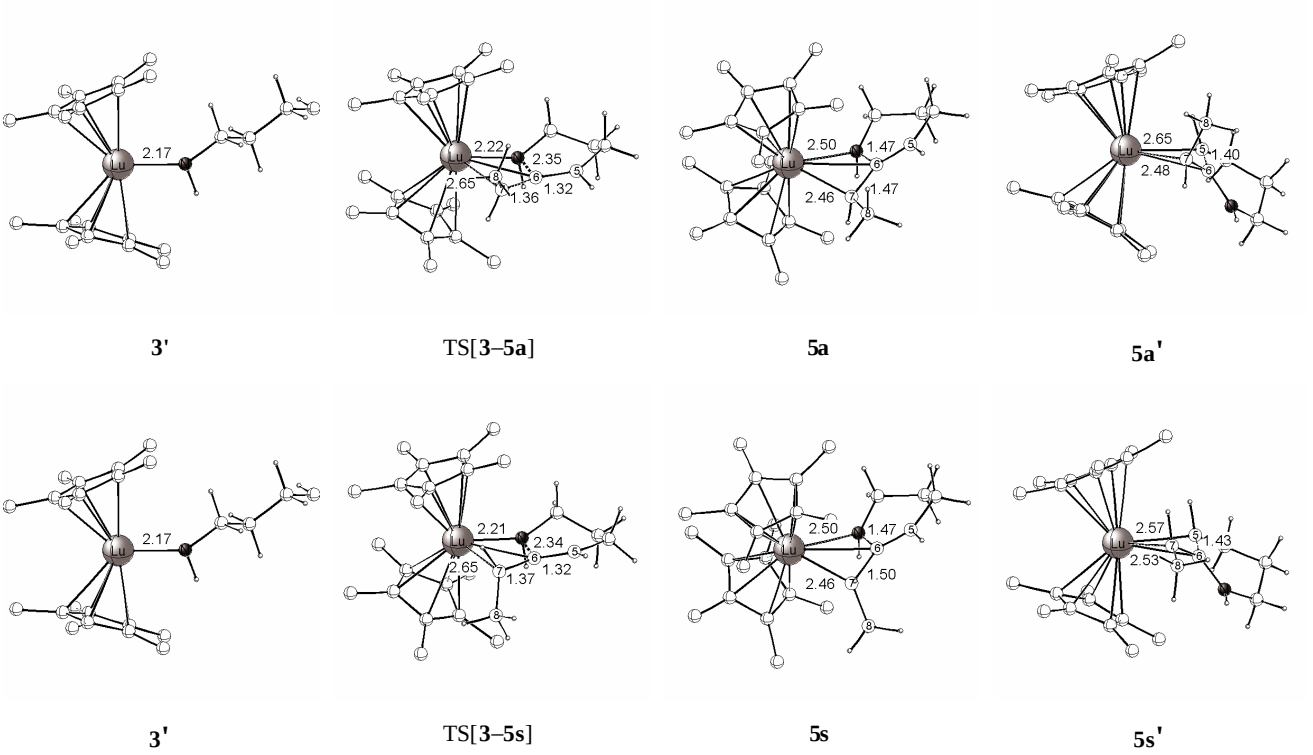

3' TS[**3**–**5a**] **5a** **5a'**

3' TS[**3**–**5s**] **5s** **5s'**

Figure S2. Selected structural parameter [Å] of the optimized structures of key species for *anti* (top) and *syn* (bottom) pathways of 6-*endo* cyclization. The cutoff for drawing Lu–C bonds was arbitrarily set to 3.1 Å. The hydrogen atoms on the methyl groups of the catalyst backbone are omitted for the sake of clarity. Please note that the amino-/amidoallene moiety and the catalyst's backbone are displayed in a truncated fashion for several of the species.

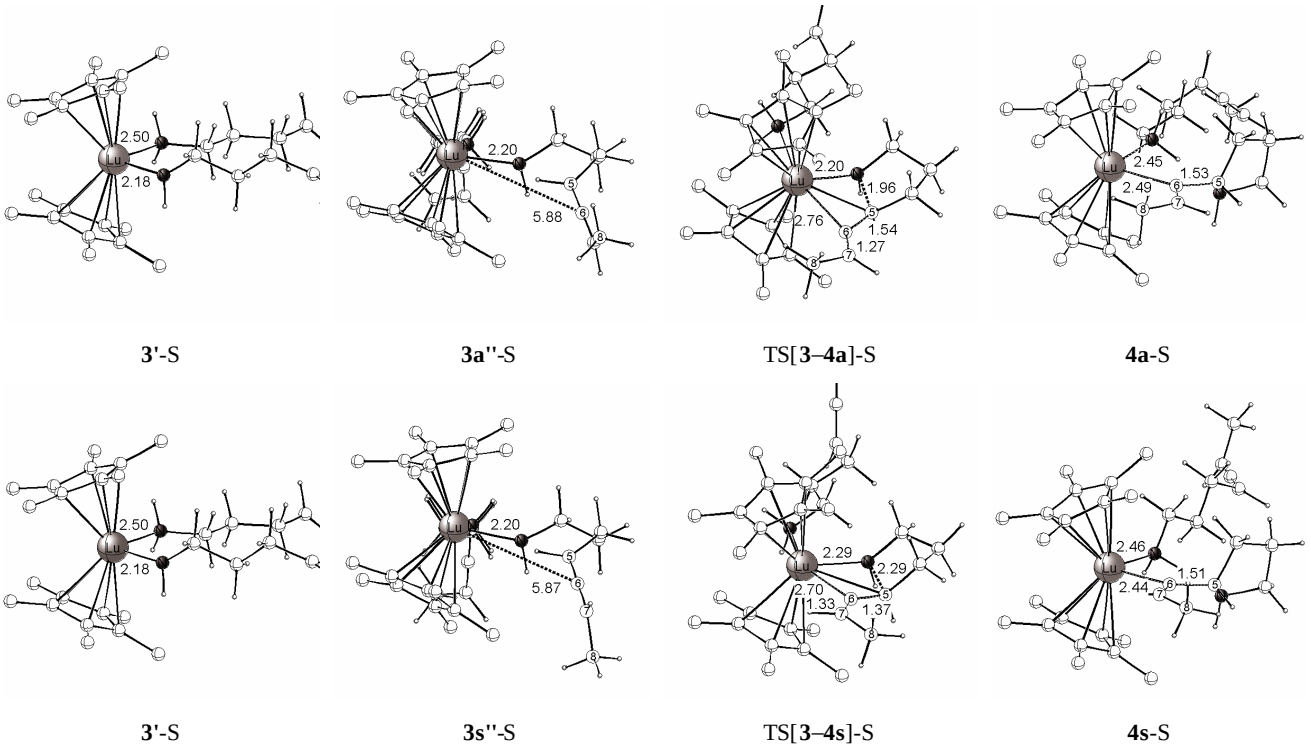

3'-S **3a''**-S TS[**3**–**4a**]-S **4a**-S

3'-S **3s''**-S TS[**3**–**4s**]-S **4s**-S

Figure S3. Selected structural parameter [Å] of the optimized structures of key species for *anti* (top) and *syn* (bottom) pathways of 5-*exo* cyclization to be assisted by aminoallene substrate **1**. The cutoff for drawing Lu–C bonds was arbitrarily set to 3.1 Å. The hydrogen atoms on the methyl groups of the catalyst backbone are omitted for the sake of clarity. Please note that the amino-/amidoallene moiety and the catalyst's backbone are displayed in a truncated fashion for several of the species.

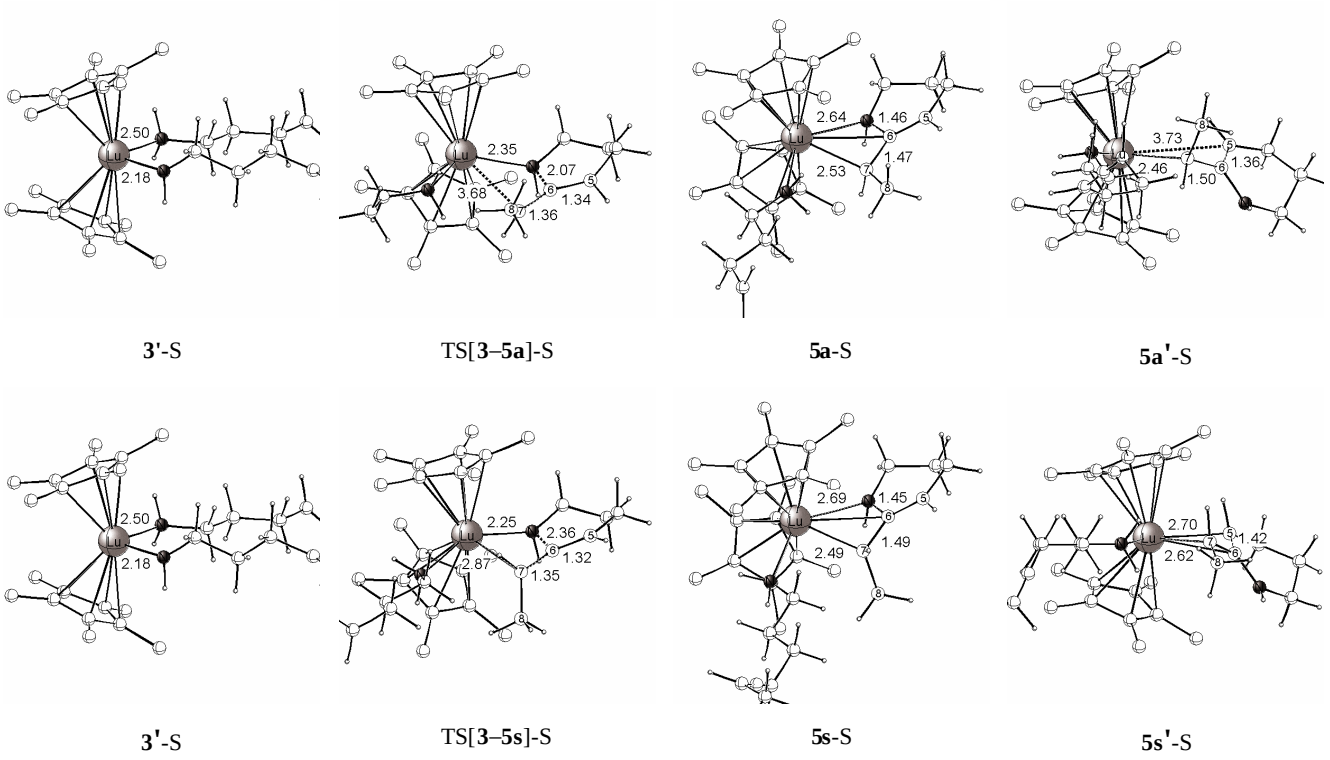

3'-S TS[**3**–**5a**]-S **5a**-S **5a'**-S

3'-S TS[**3**–**5s**]-S **5s**-S **5s'**-S

Figure S4. Selected structural parameter [Å] of the optimized structures of key species for *anti* (top) and *syn* (bottom) pathways of 6-*endo* cyclization to be assisted by aminoallene substrate **1**. The cutoff for drawing Lu–C bonds was arbitrarily set to 3.1 Å. The hydrogen atoms on the methyl groups of the catalyst backbone are omitted for the sake of clarity. Please note that the amino-/amidoallene moiety and the catalyst's backbone are displayed in a truncated fashion for several of the species.

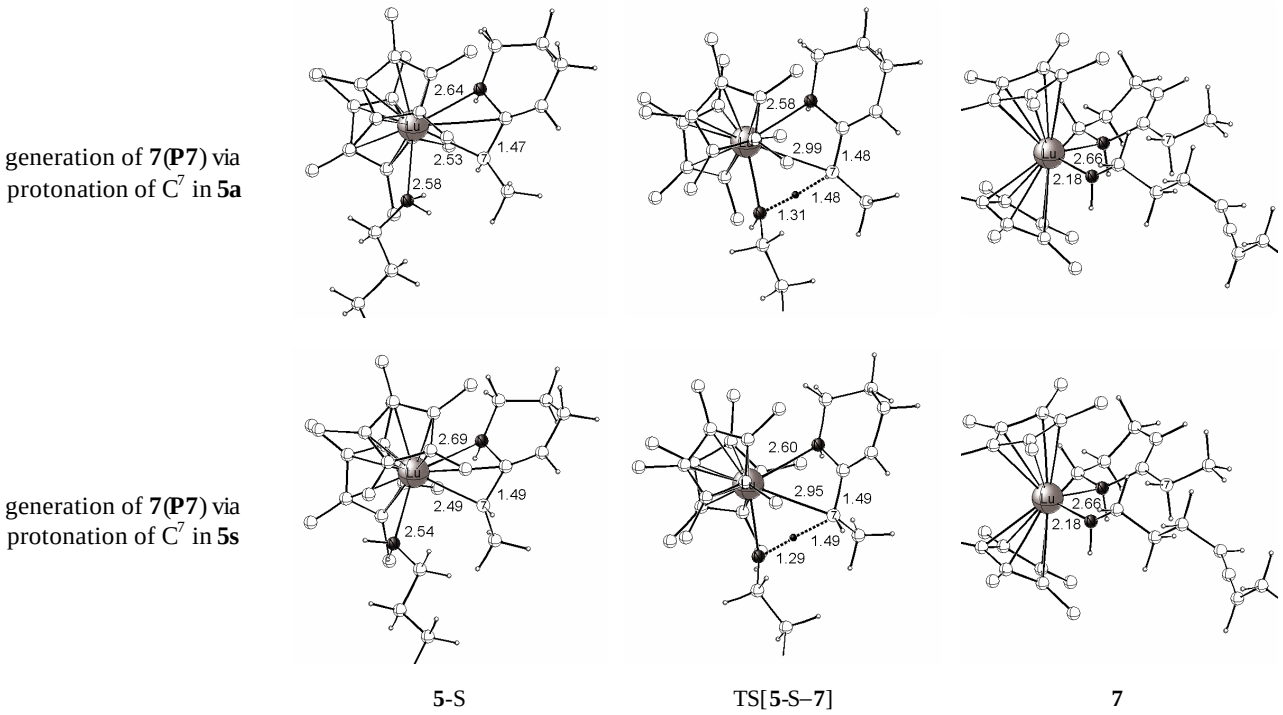

Figure S5. Selected structural parameter [Å] of the optimized structures of key species for protonolysis of the azacycle–Lu intermediate **5** by aminoallene substrate **1** affording the cycloamine-amido–Lu compound **7** along alternative pathways. The cutoff for drawing Lu–C bonds was arbitrarily set to 3.1 Å. The hydrogen atoms on the methyl groups of the catalyst backbone are omitted for the sake of clarity. Please note that the amino-/amidoallene moiety and the catalyst's backbone are displayed in a truncated fashion for several of the species.

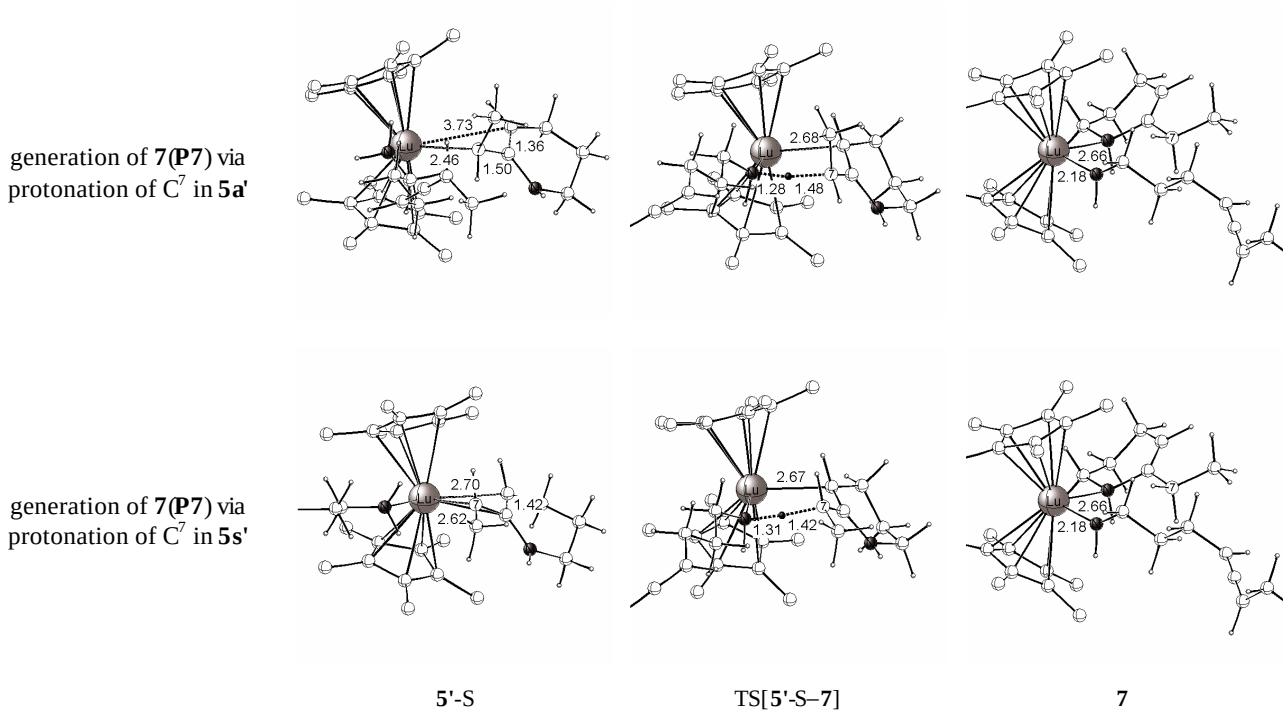

Figure S6. Selected structural parameter [Å] of the optimized structures of key species for protonolysis of the azacycle–Lu intermediate **5'** by aminoallene substrate **1** affording the cycloamine-amido–Lu compound **7** along alternative pathways. The cutoff for drawing Lu–C bonds was arbitrarily set to 3.1 Å. The hydrogen atoms on the methyl groups of the catalyst backbone are omitted for the sake of clarity. Please note that the amino-/amidoallene moiety and the catalyst's backbone are displayed in a truncated fashion for several of the species.

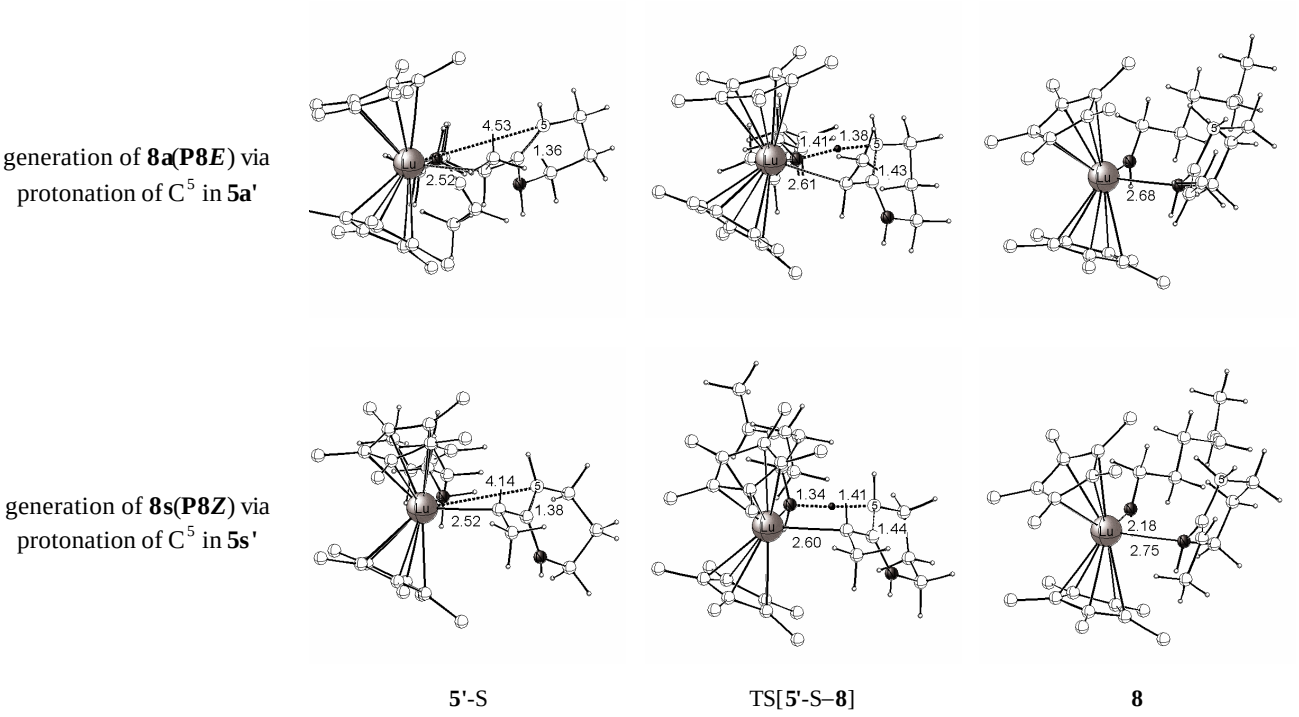

Figure S7. Selected structural parameter [Å] of the optimized structures of key species for protonolysis of the azacycle–Lu intermediate **5'** by aminoallene substrate **1** affording the cycloamine-amido–Lu compounds **8a**, **8s** along alternative pathways. The cutoff for drawing Lu–C bonds was arbitrarily set to 3.1 Å. The hydrogen atoms on the methyl groups of the catalyst backbone are omitted for the sake of clarity. Please note that the amino-/amidoallene moiety and the catalyst's backbone are displayed in a truncated fashion for several of the species.

generation of **6a**(**P6*E***) via protonation of C^6 in **4a**

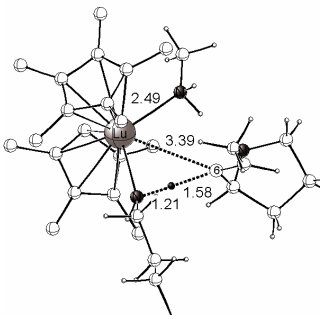

TS[**4**-S–**6**]-$MeNH_2$

generation of **6s**(**P6*Z***) via protonation of C^6 in **4s**

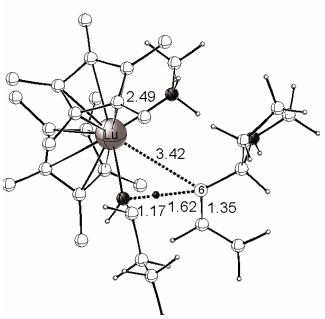

TS[**4**-S–**6**]-$MeNH_2$

generation of **6a**(**P6*E***) via protonation of C^6 in **4a**

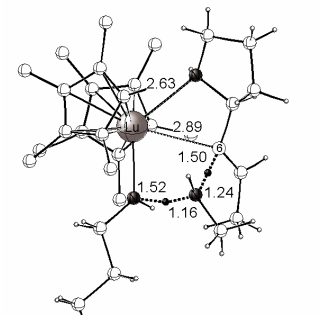

TS[**4**-S-$MeNH_2$–**6**]

generation of **6s**(**P6*Z***) via protonation of C^6 in **4s**

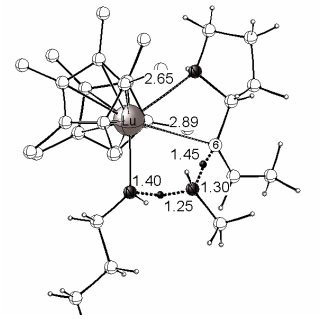

TS[**4**-S-$MeNH_2$–**6**]

Figure S8. Selected structural parameter [Å] of the optimized transition-state structures for protonolysis of the azacycle–Lu intermediate **4** by aminoallene substrate **1** affording the cycloamine-amido–Lu compounds **6a**, **6s** along alternative pathways that are assisted by methylamine model substrate, with the additive substrate to act as a coordinated spectator ligand (top) or as a 'proton shuttle' (bottom). The cutoff for drawing Lu–C bonds was arbitrarily set to 3.1 Å. The hydrogen atoms on the methyl groups of the catalyst backbone are omitted for the sake of clarity. Please note that the amino-/amidoallene moiety and the catalyst's backbone are displayed in a truncated fashion for several of the species.

generation of **7**(**P7**) via protonation of C^7 in **5a'**

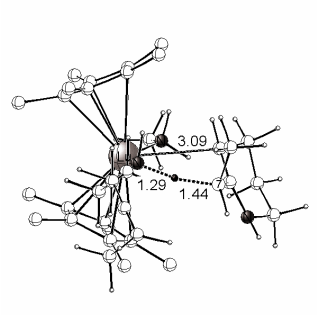

TS[**5'**-S–**7**]-$MeNH_2$

generation of **7**(**P7**) via protonation of C^7 in **5s'**

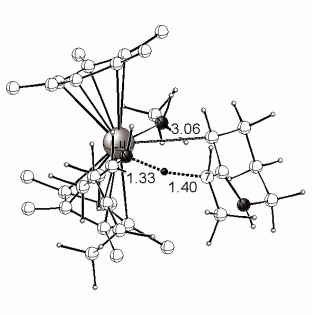

TS[**5'**-*S*–**7**]-$MeNH_2$

generation of **7**(**P7**) via protonation of C^7 in **5a'**

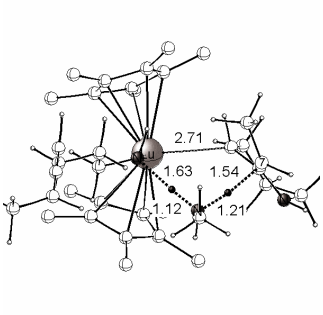

TS[**5'**-S-$MeNH_2$–**7**]

generation of **7**(**P7**) via protonation of C^7 in **5s'**

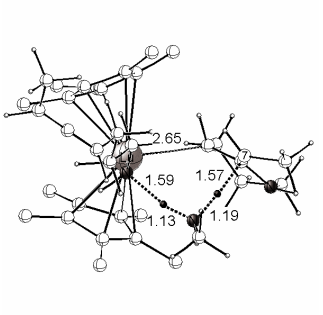

TS[**5'**-*S*-$MeNH_2$–**7**]

Figure S9. Selected structural parameter [Å] of the optimized transition-state structures for protonolysis of the azacycle–Lu intermediate **5'** by aminoallene substrate **1** affording the cycloamine-amido–Lu compound **7** along alternative pathways that are assisted by methylamine model substrate, with the additive substrate to act as a coordinated spectator ligand (top) or as a 'proton shuttle' (bottom). The cutoff for drawing Lu–C bonds was arbitrarily set to 3.1 Å. The hydrogen atoms on the methyl groups of the catalyst backbone are omitted for the sake of clarity. Please note that the amino-/amidoallene moiety and the catalyst's backbone are displayed in a truncated fashion for several of the species.

generation of **8a**(**P8*E***) via protonation of C^5 in **5a'**

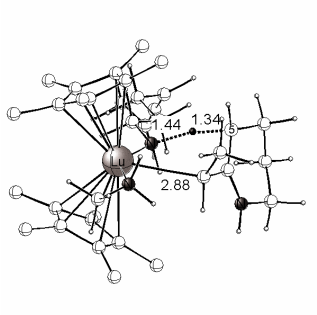

TS[**5'**-S–**8**]-$MeNH_2$

generation of **8s**(**P8*Z***) via protonation of C^5 in **5s'**

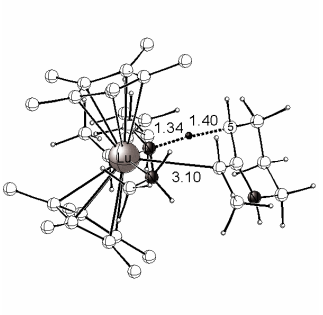

TS[**5'**-S–**8**]-$MeNH_2$

generation of **8a**(**P8*E***) via protonation of C^5 in **5a'**

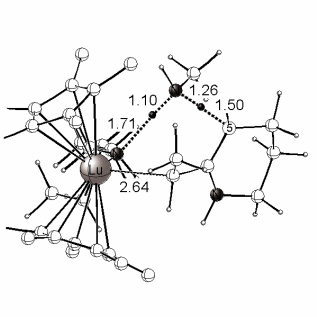

TS[**5'**-S-$MeNH_2$–**8**]

generation of **8s**(**P8*Z***) via protonation of C^5 in **5s'**

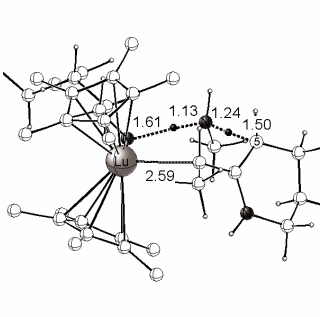

TS[**5'**-S-$MeNH_2$–**8**]

Figure S10. Selected structural parameter [Å] of the optimized transition-state structures for protonolysis of the azacycle–Lu intermediate **5'** by aminoallene substrate **1** affording the cycloamine-amido–Lu compounds **8a**, **8s** along alternative pathways that are assisted by methylamine model substrate, with the additive substrate to act as a coordinated spectator ligand (top) or as a 'proton shuttle' (bottom). The cutoff for drawing Lu–C bonds was arbitrarily set to 3.1 Å. The hydrogen atoms on the methyl groups of the catalyst backbone are omitted for the sake of clarity. Please note that the amino-/amidoallene moiety and the catalyst's backbone are displayed in a truncated fashion for several of the species.